JCI The Journal of Clinical Investigation

Nuclear receptor/microRNA circuitry links muscle fiber type to energy metabolism

Zhenji Gan, … , Anastasia Kralli, Daniel P. Kelly

J Clin Invest. 2013;123(6):2564-2575. https://doi.org/10.1172/JCI67652.

Research Article **Muscle biology**

The mechanisms involved in the coordinate regulation of the metabolic and structural programs controlling muscle fitness and endurance are unknown. Recently, the nuclear receptor PPARβ/δ was shown to activate muscle endurance programs in transgenic mice. In contrast, muscle-specific transgenic overexpression of the related nuclear receptor, PPARα, results in reduced capacity for endurance exercise. We took advantage of the divergent actions of PPARβ/δ and PPARα to explore the downstream regulatory circuitry that orchestrates the programs linking muscle fiber type with energy metabolism. Our results indicate that, in addition to the well-established role in transcriptional control of muscle metabolic genes, PPARβ/δ and PPARα participate in programs that exert opposing actions upon the type I fiber program through a distinct muscle microRNA (miRNA) network, dependent on the actions of another nuclear receptor, estrogen-related receptor γ (ERRγ). Gain-of-function and loss-of-function strategies in mice, together with assessment of muscle biopsies from humans, demonstrated that type I muscle fiber proportion is increased via the stimulatory actions of ERRγ on the expression of miR-499 and miR-208b. This nuclear receptor/miRNA regulatory circuit shows promise for the identification of therapeutic targets aimed at maintaining muscle fitness in a variety of chronic disease states, such as obesity, skeletal myopathies, and heart failure.

Nuclear receptor/microRNA circuitry links muscle fiber type to energy metabolism

Zhenji Gan,[1] John Rumsey,[1] Bethany C. Hazen,[2] Ling Lai,[1] Teresa C. Leone,[1] Rick B. Vega,[1] Hui Xie,[3] Kevin E. Conley,[4] Johan Auwerx,[5] Steven R. Smith,[1,3] Eric N. Olson,[6] Anastasia Kralli,[2] and Daniel P. Kelly[1]

[1]Diabetes and Obesity Research Center, Sanford-Burnham Medical Research Institute, Orlando, Florida, USA. [2]Department of Chemical Physiology, The Scripps Research Institute, La Jolla, California, USA. [3]Translational Research Institute for Metabolism and Diabetes, Florida Hospital, Orlando, Florida, USA. [4]Departments of Radiology, Physiology and Biophysics, and Bioengineering, University of Washington Medical Center, Seattle, Washington, USA. [5]Laboratory of Integrative and Systems Physiology, École Polytechnique Fédérale de Lausanne, Lausanne, Switzerland. [6]Department of Molecular Biology, University of Texas Southwestern Medical Center, Dallas, Texas, USA.

The mechanisms involved in the coordinate regulation of the metabolic and structural programs controlling muscle fitness and endurance are unknown. Recently, the nuclear receptor PPARβ/δ was shown to activate muscle endurance programs in transgenic mice. In contrast, muscle-specific transgenic overexpression of the related nuclear receptor, PPARα, results in reduced capacity for endurance exercise. We took advantage of the divergent actions of PPARβ/δ and PPARα to explore the downstream regulatory circuitry that orchestrates the programs linking muscle fiber type with energy metabolism. Our results indicate that, in addition to the well-established role in transcriptional control of muscle metabolic genes, PPARβ/δ and PPARα participate in programs that exert opposing actions upon the type I fiber program through a distinct muscle microRNA (miRNA) network, dependent on the actions of another nuclear receptor, estrogen-related receptor γ (ERRγ). Gain-of-function and loss-of-function strategies in mice, together with assessment of muscle biopsies from humans, demonstrated that type I muscle fiber proportion is increased via the stimulatory actions of ERRγ on the expression of miR-499 and miR-208b. This nuclear receptor/miRNA regulatory circuit shows promise for the identification of therapeutic targets aimed at maintaining muscle fitness in a variety of chronic disease states, such as obesity, skeletal myopathies, and heart failure.

Introduction

Muscle fitness is an important determinant of health and disease. Muscle endurance, strength, and fatigability are determined by a variety of factors, including delivery of substrate for ATP production, mitochondrial capacity to burn fuels, and composition of the contractile machinery (1–3). Although genetic factors serve to determine the fundamental muscle phenotype, physiological factors such as physical activity and exercise also contribute during the postnatal period through effects on fiber-type composition, mitochondrial biogenesis, and energy metabolic pathways.

Muscle fibers can be broadly classified as slow twitch (type I) and fast twitch (type II). Type I fibers are mitochondria-rich, relying largely on mitochondrial fatty acid oxidation for ATP production. Type II fibers rely on glucose as an energy substrate and are subclassified as type IIa, IIx, or IIb in rodents based on the type of myosin heavy chain (MHC) isoform expressed (4, 5). Whole-body insulin sensitivity and insulin-stimulated glucose transport are positively correlated with the proportion of type I muscle fibers (6–9). Endurance exercise training increases the proportion of oxidative fibers in parallel with a mitochondrial biogenic response, which, in turn, increases capacity for exercise, oxidation of fatty acids and glucose, and energy expenditure (1–3, 10). Conversely, reduced physical activity, such as occurs in obese states and chronic illness, results in a reduction in the proportion of type I and IIa fibers, along with reduced muscle glucose disposal and insulin sensitivity (11, 12).

The mechanisms involved in the coordinate regulation of the metabolic and structural determinants of muscle fitness and endurance during development and in response to physiological stimuli are unknown. Recent studies in muscle-specific transgenic mice have provided important clues. Mice overexpressing the transcriptional coactivator PGC-1α exhibit increased muscle mitochondrial density and respiratory capacity, a greater proportion of oxidative muscle fibers, and enhanced exercise performance (13). Muscle-specific transgenes for the nuclear receptor PPARβ/δ also exhibit a "trained" phenotype, in which both energy metabolic and fiber-type programs linked to muscle endurance are activated, in the absence of exercise (14–16). In contrast, we recently found that muscle-specific transgenic overexpression of a related nuclear receptor, PPARα (MCK-PPARα mice), results in reduced endurance (16, 17).

The strikingly different muscle phenotypes of PPARα and PPARβ/δ transgenic mice suggested that the circuitry involved in the control of muscle endurance is differentially regulated in the two lines. We took advantage of the divergent actions of PPARβ/δ and PPARα in muscle to explore the downstream regulatory circuitry that coordinately regulates muscle fiber type and energy metabolism (16). We found that, in addition to the well-established role in the transcriptional control of energy metabolic genes, PPARβ/δ and PPARα participate in programs that exert opposing actions upon the slow-twitch type I fiber program

Conflict of interest: Daniel P. Kelly is on scientific advisory boards for Pfizer and Lilly and has received research funds from Takeda Pharmaceuticals. Eric N. Olson holds equity in miRagen Therapeutics, which is developing miRNA-based therapies for heart and muscle disease. Steven R. Smith has received research funds from Novartis Clinical Innovation Fund and Takeda Pharmaceuticals.

Note regarding evaluation of this manuscript: Manuscripts authored by scientists associated with Duke University, The University of North Carolina at Chapel Hill, Duke-NUS, and the Sanford-Burnham Medical Research Institute are handled not by members of the editorial board but rather by the science editors, who consult with selected external editors and reviewers.

Citation for this article: *J Clin Invest.* 2013;123(6):2564–2575. doi:10.1172/JCI67652.

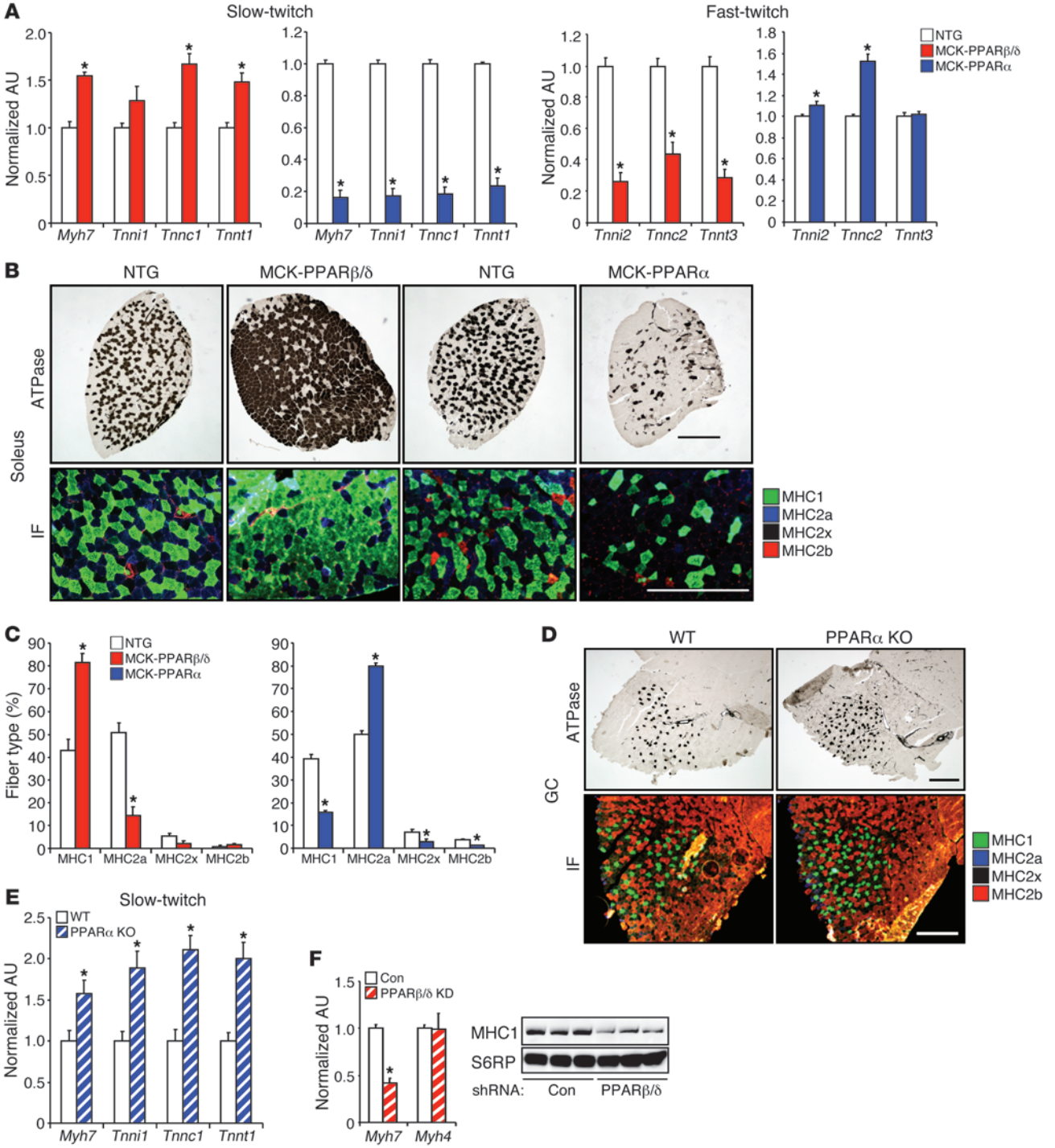

Figure 1

PPARβ/δ and PPARα regulate opposing muscle fiber-type programs. (**A**) Expression of the slow-twitch myosin *Myh7* and representative slow/fast-twitch troponin genes (qRT-PCR) in soleus muscle from indicated genotypes (n = 5–13 mice per group). (**B**) Cross-section of soleus muscle from 3- to 4-month-old male MCK-PPARβ/δ and MCK-PPARα mice (n = 5 mice per group) stained for myosin I ATPase activity as well as MHC fiber typing by immunofluorescence (IF) of soleus of indicated genotypes (MHC1 [green], MHC2a [blue], MHC2b [red], and MHC2x [unstained]). Scale bar: 500 μm. (**C**) Quantification of immunofluorescence data shown in **B** expressed as mean percentage total muscle fibers. (**D**) Muscle fiber typing in GC of WT and PPARα-null (PPARα KO) mice (n = 5 mice per group) as described in **B**. Scale bar: 500 μm. (**E**) Quantification of contractile protein gene expression in GC from indicated genotypes (n = 6–9 mice per group). (**F**) qRT-PCR results and Western blot analysis of *Myh* expression in skeletal myotubes harvested from WT mice subjected to adenovirus-based overexpression of PPARβ/δ shRNA (KD) compared with control shRNA (con) (n = 3). *P < 0.05 vs. corresponding controls. All values represent mean ± SEM and are shown as arbitrary units (AU) normalized to corresponding controls.

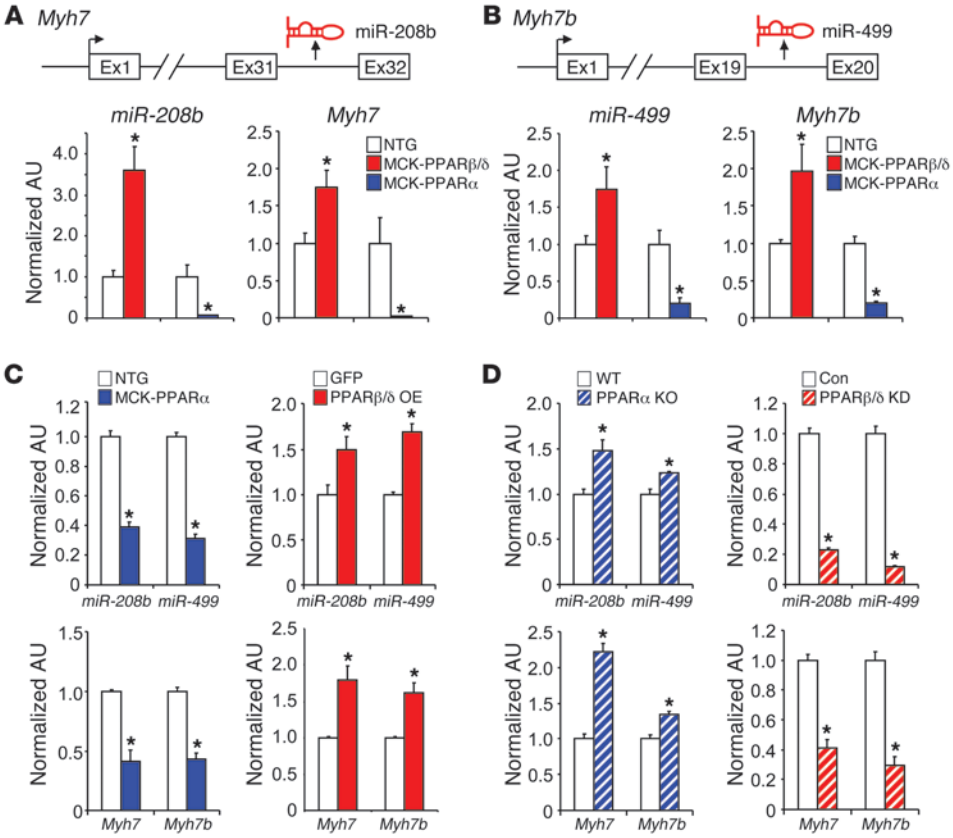

Figure 2
PPARβ/δ and PPARα control distinct miRNA subnetworks in skeletal muscle. (**A** and **B**) qRT-PCR analysis of *Myh7*/*miR-208b* and *Myh7b*/*miR-499* levels in GC muscles of indicated genotypes (n = 5–8 mice per group). Schematics at the top indicate the location of the *miR-208b* and *miR-499* genes within the *Myh7* and *Myh7b* genes. Exons are denoted in the boxes. (**C** and **D**) Mean expression levels (qRT-PCR) in myotubes harvested from GC of WT mice or indicated genotypes subjected to adenovirus-based overexpression (OE) of PPARβ/δ compared with GFP control or shRNA-mediated KD of PPARβ/δ compared with control shRNA (con) (n = 3). *P < 0.05 vs. corresponding controls. All values represent mean ± SEM and are shown as arbitrary units normalized to corresponding controls.

through a distinct muscle microRNA (miRNA) network. Our studies also strongly suggest that the estrogen-related receptor γ/miRNA (ERRγ/miRNA) circuitry is operational in human muscle.

Results

MCK-PPAR transgenic lines exhibit strikingly different muscle fiber-type phenotypes. The distinct exercise phenotypes of the two MCK-PPAR lines (16) afforded us the opportunity to use a comparative molecular profiling strategy to identify gene regulatory networks involved in the coordinate control of muscle energy metabolism and fiber type. Muscle phenotyping and transcriptional profiling revealed that fiber-type programs are differentially regulated, at the gene regulatory level, in the MCK-PPAR lines; expression of type I genes is increased in MCK-PPARβ/δ muscle but is decreased in MCK-PPARα muscle (Supplemental Table 1; supplemental material available online with this article; doi:10.1172/JCI67652DS1). Gene expression validation studies demonstrated that the expression of the gene encoding the major slow-twitch type I myosin isoform MHC1 (*Myh7* gene) and slow-twitch troponin genes was increased in MCK-PPARβ/δ soleus muscle, concomitant with a reduction in the expression of the MHC2a (*Myh2*), MHC2x (*Myh1*), and MHC2b (*Myh4*) genes (Figure 1A and data not shown). In striking contrast, expression of *Myh7* and slow-twitch troponin genes was reduced in MCK-PPARα soleus muscle (Figure 1A). Similar observations were made in gastrocnemius (GC) muscles of the MCK-PPAR lines (Supplemental Figure 1, A and B). Consistent with the gene expression results, metachromatic ATPase and MHC immunostaining demonstrated an increase in MHC1-positive (type I) fibers in MCK-PPARβ/δ muscle but a marked reduction of MHC1-positive fibers in MCK-PPARα muscle (Figure 1, B and C). These results were not due to differences in spontaneous locomotor activity, muscle size, or fiber density of the MCK-PPAR lines compared with nontransgenic (NTG) littermate controls (data not shown).

Loss-of-function experiments were conducted to determine whether PPAR signaling is required for normal muscle fiber-type programming. MHC1-positive muscle fibers were significantly increased, together with elevated expression of slow-twitch troponin genes, in GC muscles of PPARα-null mice compared with those in controls (Figure 1, D and E). However, type I fiber proportion was normal in PPARα-null soleus (data not shown), suggesting the existence of redundant pathways in this muscle. In vitro manipulation of PPARα or PPARβ/δ levels in a primary skeletal myocyte culture system further demonstrated that the two nuclear receptors exert opposing effects on *Myh7* expression (Figure 1F and Supplemental Figure 2, A and B). Taken together, these data demonstrate essential and opposing roles of PPARβ/δ and PPARα in the regulation of type I muscle fiber type.

PPAR signaling exerts control upon muscle fiber type through a specific miRNA network. Evidence is emerging that coordinate modulation of gene regulatory circuits is often directed by miRNAs (18). Therefore, unbiased muscle miRNA profiling was conducted, unveiling interesting differences between the MCK-PPAR lines (Supplemental Figure 3). Two miRNAs implicated previously in muscle fiber-type programs (19) were differentially regulated: miR-208b, which is encoded within the *Myh7* gene, and miR-499, which is encoded within the *Myh7b* gene. miR-499 and miR-208b, which target the same mRNA targets, have been shown to drive a slow-twitch program by downregulating transcriptional repressors of slow-twitch contractile protein genes, such as *Sox6* (19, 20). Expression of miR-

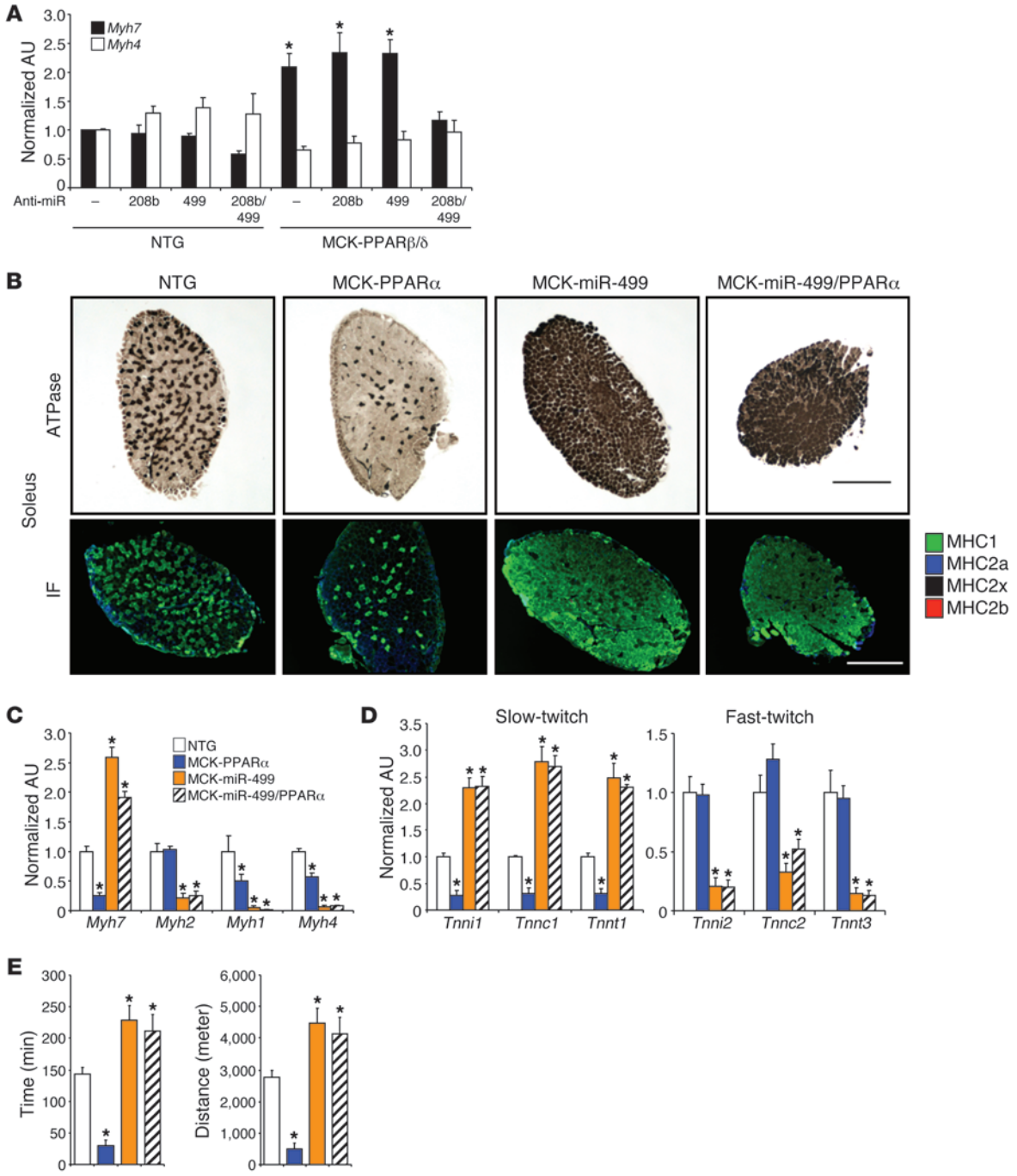

Figure 3

miR-208b and miR-499 mediate opposing effects of PPARβ/δ and PPARα on muscle fiber-type determination. (**A**) qRT-PCR analysis of *Myh7* and *Myh4* transcripts in myotubes harvested from muscles of MCK-PPARβ/δ and NTG mice subjected to inhibition of miR-208b and/or miR-499 ($n = 4$). (–), negative control anti-miR. (**B**) Muscle fiber typing, as described in the legend for Figure 1B, of soleus muscle from indicated genotypes ($n = 5$ mice per group). Scale bar: 500 μm. (**C** and **D**) Gene expression (qRT-PCR) in soleus muscle from indicated genotypes ($n = 5$–8 mice per group). (**E**) Mean running time and distance for indicated genotypes during endurance exercise on a motorized treadmill ($n = 5$–7 mice per group). *$P < 0.05$ vs. NTG. One-way ANOVA was used for statistics. All values represent mean ± SEM and are shown as arbitrary units normalized to corresponding controls.

208b was significantly increased in MCK-PPARβ/δ muscle but was undetectable in MCK-PPARα muscle (Figure 2A and Supplemental Figure 3). In addition, miR-499 expression was increased in MCK-PPARβ/δ muscle but dramatically reduced in MCK-PPARα muscle (Figure 2B and Supplemental Figure 3). Similar results were obtained in skeletal myocytes in culture, using either transgenic cells or adenoviral-mediated PPAR overexpression in WT myocytes (Figure 2C, top). Furthermore, *miR-208b* and *miR-499*

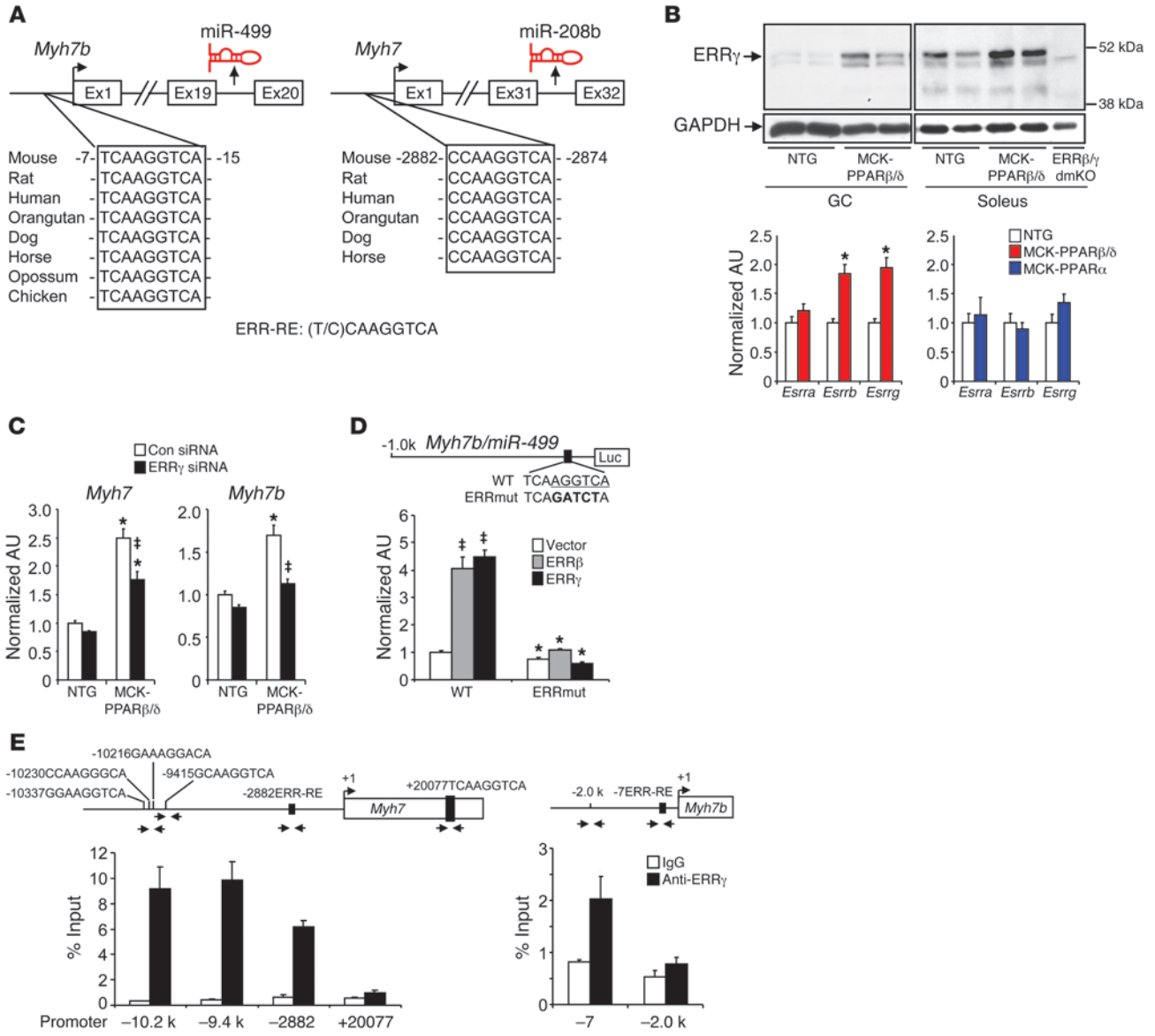

Figure 4

PPARβ/δ and ERRγ function cooperatively to control miR-208b and miR-499 expression. (**A**) The putative conserved ERR binding site within the *Myh7* and *Myh7b* promoter regions. (**B**) ERR mRNA (GC, bottom) and ERRγ protein (GC and soleus, top) expression in muscle from indicated genotypes (n = 6–15 mice per group). (**C**) *Myh* transcript levels in myotubes harvested from muscles of MCK-PPARβ/δ and NTG mice subjected to ERRγ siRNA or scrambled control (Con) (n = 4). (**D**) Site-directed mutagenesis was used to abolish the ERR response element (top). The m*Myh7b*.Luc.1K (WT) or ERRmut.m*Myh7b*.Luc.1K promoter-reporters were used in cotransfection studies in C2C12 myotubes in the presence or absence of ERRβ or ERRγ (n = 3) (bottom). (**E**) Results of SYBR green–based quantification of ERRγ ChIP assays performed on WT primary mouse myotubes (n = 3). The graphs show enrichment relative (%) to input, while the schematics show PCR primer set location and the location of the putative conserved ERR binding sites relative to the *Myh7* and *Myh7b* gene transcription start site (+1): –2882ERR-RE and –7ERR-RE (described in **A**) and a previously identified +20077ERR-RE (23) were analyzed. PCR primer sets located in the 2.0-kb (–2.0k) region upstream of the *Myh7b* promoter transcription start site were used as a negative control. –10.2 k, –9.4 k, –2882, +20077, and –7 represent locations in the promoter regions corresponding to the transcription start site = +1. *P < 0.05 vs. corresponding controls; ‡P < 0.05 vs. control siRNA or vector alone. One-way ANOVA was used for statistics in **C** and **D**. All values represent mean ± SEM and are shown as arbitrary units normalized to corresponding controls.

levels were increased in PPARα-null GC muscle and cultured myocytes (Figure 2D, top, and data not shown), whereas shRNA-mediated knockdown (KD) of PPARβ/δ in WT myotubes reduced levels of *miR-208b* and *miR-499* (Figure 2D, top). As expected, the expression of the *Myh7* and *Myh7b* genes paralleled the levels of miR-208b and miR-499, respectively, in these studies (Figure 2).

We next assessed the effects of manipulating miR-208b and miR-499 levels on the PPAR-mediated control of slow fiber type. First, the impact of antisense-mediated inhibition of miR-208b and/or miR-499 on MHC gene expression was evaluated in MCK-PPARβ/δ and NTG myotubes. Whereas inhibition of either miR-208b or miR-499 alone had no effect on MHC expression, inhibition of

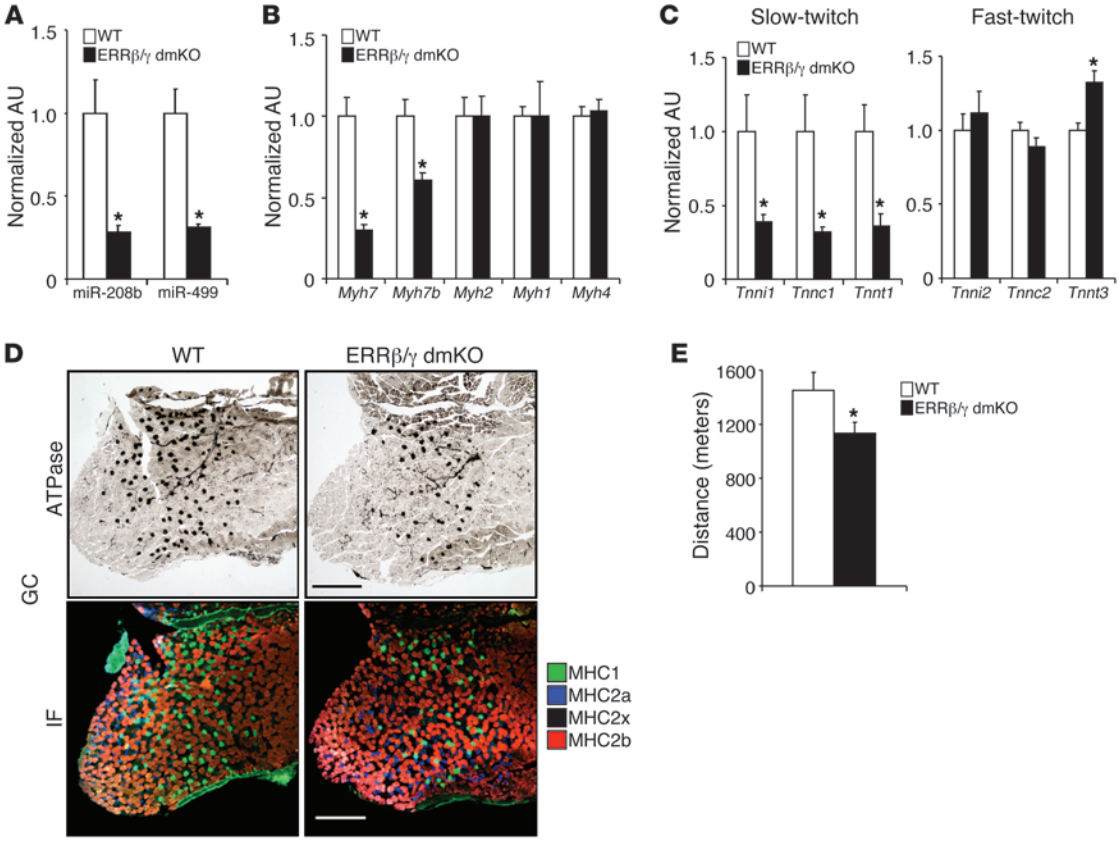

Figure 5
ERRβ/ERRγ are required for type I muscle fiber formation. (**A**) miR-208b and miR-499 levels in GC muscles of indicated genotypes (n = 6 mice per group). (**B** and **C**) Gene expression (qRT-PCR) in GC muscles from indicated genotypes (n = 6–10 mice per group). (**D**) Muscle fiber typing, as described in the legend for Figure 1B, of GC of WT and skeletal muscle–specific ERRγ/ERRβ double-deficient mice (n = 5–7 mice per group). Scale bar: 500 μm. (**E**) Mean distance (meters) traveled by 14-week-old female ERRβ/γ dmKO mice and control littermates during endurance (run-to-exhaustion) exercise on a motorized treadmill (n = 14 mice per group). *P < 0.05 vs. corresponding controls. All values represent mean ± SEM and are shown as arbitrary units normalized to corresponding controls.

both miRNAs resulted in a significant decrease in *Myh7* mRNA in WT myotubes and abolished the enhancing effects of PPARβ/δ on slow-twitch gene expression in MCK-PPARβ/δ myotubes (Figure 3A). Second, to assess the relevance of this pathway in vivo, muscle-specific miR-499 transgenic mice (MCK-miR-499 mice) were bred with the MCK-PPARα line. The resultant cross prevented the PPARα-mediated repression of the type I muscle fiber-type program (Figure 3, B–D) and reversed the exercise performance deficit of the MCK-PPARα mice (Figure 3E). Taken together, these results support a model in which PPAR signaling is upstream of miR-208b/miR-499 and that PPARβ/δ activates, whereas PPARα suppresses, *Myh7/miR-208b* and *Myh7b/miR-499* expression in muscle.

The nuclear receptor ERRγ functions downstream of PPARβ/δ to activate transcription of Myh7/miR-208b and Myh7b/miR-499 in muscle. We next sought to determine the mechanism whereby the *Myh7/miR-208b* and *Myh7b/miR-499* transcripts were upregulated in the MCK-PPARβ/δ line. Analysis of the *Myh7/miR-208b* and *Myh7b/miR-499* promoter regions did not reveal consensus PPAR binding sites. However, highly conserved sequences that conformed to the consensus binding sites for ERR were identified in both promoter regions (Figure 4A). The putative *Myh7* ERR binding site is located well upstream of the well-described proximal promoter elements known to respond to the thyroid receptor, MCAT, and Sox6 (20, 21). Notably, ERRγ has been shown recently to activate oxidative muscle fiber programs in a manner similar to that of PPARβ/δ (14, 22). We found that ERRγ (*Esrrg*) mRNA and protein levels were increased in MCK-PPARβ/δ muscle but not in MCK-PPARα muscle (Figure 4B and data not shown). ERRβ (*Esrrb*), but not ERRα (*Esrra*), expression was also increased in MCK-PPARβ/δ muscle (Figure 4B). In contrast, the expression of the genes encoding PGC-1α and PGC-1β, known activators of muscle endurance, was not increased in MCK-PPARβ/δ muscle compared with that in controls (Supplemental Figure 4A). siRNA-mediated KD of ERRγ attenuated the PPARβ/δ-mediated activation of *Myh7* and *Myh7b* transcript levels (Figure 4C). In addition, ERRγ and ERRβ activated a 1-kb mouse *Myh7b* promoter-reporter via the ERR site in C2C12 myotubes (Figure 4D). Interestingly, PGC-1α, when overexpressed in cells, did not have a coactivating effect on ERRγ, using the *Myh7b* promoter-reporter as a readout (Supplemental Figure 4B). ChIP studies confirmed that ERRγ occupies the regions of the *Myh7* and *Myh7b* promoters containing the ERR-responsive elements (Figure 4E). In addition, ERRγ occupied a putative regulatory region (based on ENCODE/LICR data in the UCSC Genome Browser) containing multiple conserved ERR response elements, approximately 10 kb

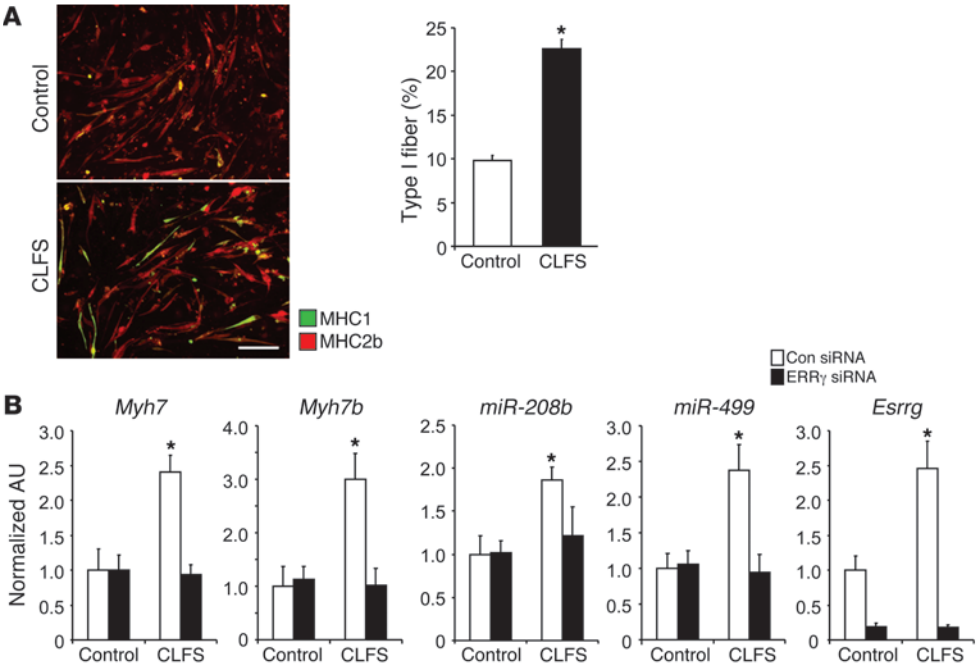

Figure 6
The ERRγ/miRNA circuit is induced by CLFS in skeletal myotubes in culture. (**A**) MHC fiber typing by immunofluorescence in CLFS or unstimulated myotubes (MHC1 [green], MHC2b [red]). Scale bar: 200 μm. Quantification of the immunofluorescence data shown on the left expressed as mean percentage total myotubes (n = 5). (**B**) qRT-PCR analysis of *Myh7/miR-208b*, *Myh7b/miR-499*, and *Esrrg* levels in CLFS and unstimulated mouse myotubes subjected to ERRγ siRNA or scrambled control (Con) (n = 3). *P < 0.05 vs. corresponding controls. One-way ANOVA was used for statistics in **B**. All values represent mean ± SEM and are shown as arbitrary units normalized to corresponding controls.

upstream of the *Myh7* gene transcription initiation site (Figure 4E). Interestingly, these sites are markedly stronger than a previously identified ERR element (20077 bp downstream of the *Myh7* transcription start site) in heart (23).

To assess the role of ERR signaling in the miR-499/miR-208b–mediated control of muscle fiber type in vivo, mice with skeletal muscle–specific disruption of the *Esrrg* and *Esrrb* genes (ERRβ/γ dmKO mice) were generated and analyzed (Supplemental Figure 5). Levels of miR-499 and miR-208b were dramatically reduced in ERRβ/γ dmKO GC muscle (Figure 5A). In addition, slow-twitch fiber gene expression and MHC1-positive fibers were reduced in ERRβ/γ dmKO GC muscle (Figure 5, B–D). These results were not due to differences in the general spontaneous activity of the mice or obvious pathologic changes in the muscles of the ERRβ/γ dmKO line. Interestingly, a change in type I fiber composition was not observed in the soleus muscles of the ERRβ/γ dmKO mice (data not shown), suggesting the existence of additional converging pathways involved in the control of fiber type in this muscle.

We next assessed acute running endurance performance in the ERRβ/γ dmKO line using a run-to-exhaustion protocol on a motorized treadmill. Consistent with the observed alterations in muscle fiber-type proportion, the ERRβ/γ dmKO mice achieved a shorter distance compared with that of the WT controls (Figure 5E).

PPARα suppresses Myh7/miR-208b and Myh7b/miR-499 promoter activity. To define the mechanism by which PPARα downregulates *miR-208b* and *miR-499* gene expression, transcriptional regulation studies were conducted by transiently transfecting rat 3.5-kb *Myh7* and mouse 1.0-kb *Myh7b* promoter-reporter constructs into C2C12 myotubes. In agreement with the RNA quantification data, cotransfection of PPARα suppressed both promoters (Supplemental Figure 6A). Interestingly, this effect occurred independently of exogenously added PPARα ligand. A series of deletion mapping studies was used to demonstrate that PPARα suppresses *Myh7*/miR-208b promoter activity through a region within 408 bp upstream of the transcription initiation site (downstream of the identified ERR site) (Supplemental Figure 6B). In addition, the PPARα-mediated repression was maintained in a *Myh7b* gene promoter-reporter in which the ERR-responsive element was mutated (Supplemental Figure 6C). Taken together, these results strongly suggest that PPARα suppresses *Myh7/miR-208b* and *Myh7b/miR-499* promoter activity independent of the ERR-responsive element. Given that the responsive region does not contain a classic PPAR DNA recognition site, it is likely that this repressive effect occurs via indirect mechanisms, possibly via other transcription factors occupying this region.

Induction of the ERRγ/miRNA axis in skeletal myotubes by chronic low-frequency electrical stimulation. We next sought to determine whether this program can be activated by stimuli known to induce muscle type I fiber programs. Chronic low-frequency electrical stimulation (CLFS) of myotubes in culture has been shown to increase slow myosin gene expression and enhance contractile properties of muscle cells in culture (24–26). Therefore, we conducted experiments to determine whether the ERRγ/miRNA circuit is activated in response to CLFS in WT mouse primary skeletal myotubes. CLFS for 4 days induced an increase in proportion of type I fibers (Figure 6A) and expression of *Myh7*, *Myh7b*, *miR-499*, and *miR-208b* (Figure 6B). In contrast, the fast fiber-type gene *Myh4* was not induced by CLFS (data not shown). *Esrrg* levels, but not PPARβ/δ levels (data not shown), were also induced by CLFS (Figure 6B). Importantly, KD of ERRγ abolished the CLFS-mediated increase in *Myh7*, *Myh7b*, *miR-499*, and *miR-208b* (Figure 6B). These results further support the importance of the ERRγ/miRNA axis in type I fiber-type expression and demonstrate that it is an inducible program.

Activation of the ERRγ/miRNA axis is linked to muscle fitness in humans. To determine the relevance of the ERRγ/miRNA circuit in humans, muscle biopsies from 8 active, trained (referred to herein as "active") individuals and 17 healthy sedentary controls were analyzed. Previous analyses demonstrated that the biopsy specimens from the "active" group contain a higher percentage of type I muscle fibers compared with those from the sedentary

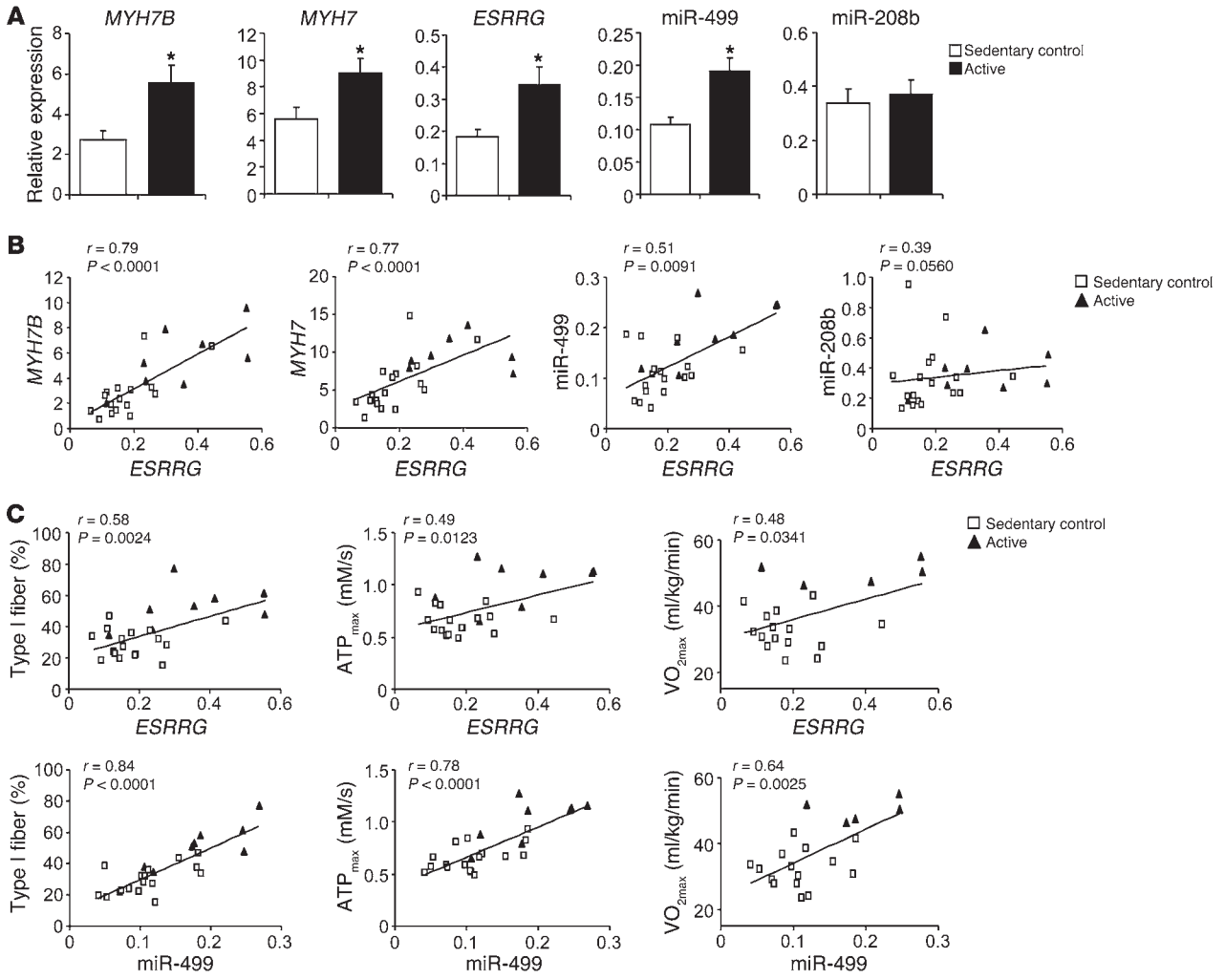

Figure 7

ERRγ/miRNA axis is associated with muscle contractile and metabolic properties in humans. Samples from 5 to 8 "active" and 15 to 17 healthy sedentary controls were used for this analysis. (**A**) mRNA expression levels of *MYH7B*, *MYH7*, *ESRRG*, miR-499, and miR-208B were determined by qRT-PCR. Data represent the mean ± SEM. Significant differences were analyzed using 2-sample *t* test. **P* < 0.05 vs. sedentary controls. (**B**) Correlation between *ESRRG* gene expression and that of muscle contractile genes, miR-499, and miR-208B. Spearman correlation analysis was used to determine the correlation. (**C**) Correlation between *ESRRG* and miR-499 expression and the type I fiber percentage, ATP_{max}, and VO_{2max}. Pearson correlation analysis was used to determine the correlation.

group (Supplemental Table 2 and ref. 27). As expected, muscle tissue from the "active" group exhibited higher slow-twitch gene (*MYH7* and *MYH7B*) expression compared with that from the sedentary control group (Figure 7A). Expression levels of *ESRRG* and miR-499 were also significantly elevated in the "active" group compared with those in the controls (Figure 7A). In addition, there was a significant positive correlation between *ESRRG* mRNA levels and both *MYH7B* and *MYH7* mRNA levels (Figure 7B). Moreover, *ESRRG* mRNA levels were positively correlated with miR-499 levels (Figure 7B). However, this correlation was not observed with miR-208B levels (Figure 7B).

The relationship between *ESRRG* expression and levels of the miRNAs with determinants of muscle endurance (type I fiber percentage, VO_{2max}, and ATP_{max}) was next assessed. As shown in Figure 7C, a strong positive correlation was observed between the expression of miR-499 and type I fiber percentage, ATP_{max}, and VO_{2max}. *ESRRG* expression also correlated with type I fiber percentage, ATP_{max}, and VO_{2max}. In contrast, the levels of *PPARD* and *PPARA* mRNA were not different between sedentary and "active" muscle, and neither exhibited a significant correlation with fiber type, ATP_{max}, or VO_{2max} (Supplemental Figure 7). Taken together, these results strongly suggest that the ERRγ/miR-499 axis is operative in the regulation of the type I muscle program in humans.

Discussion

Type I muscle fibers are equipped with a high-capacity mitochondrial system and a distinct set of contractile protein isoforms poised for endurance. The circuitry involved in the coordinate control of these seemingly distinct but highly interrelated processes is unknown. Recently, a clue was provided when the nuclear receptors PPARβ/δ and ERRγ, transcriptional regulators of cellular energy metabolism (28), were independently shown to drive

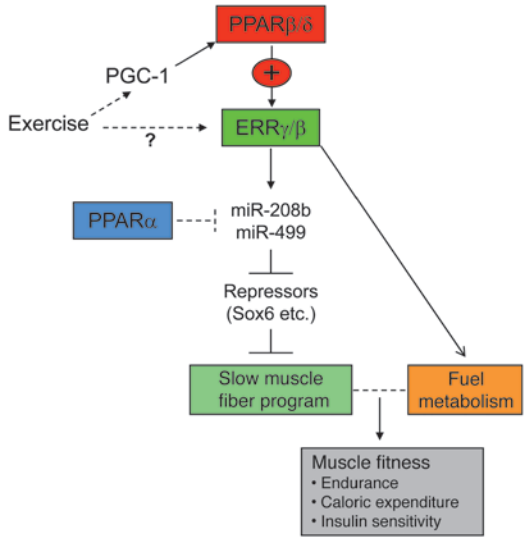

Figure 8

Model of nuclear receptor/miRNA circuit in the coordinate control of energy metabolism and muscle fiber type. The schematic depicts a proposed model for a nuclear receptor/miRNA circuit that controls muscle type I fiber-type program. ERRγ (and likely ERRβ) activates miR-208b and miR-499, triggering a type I fiber program, while PPARα suppresses the program. The effect of exercise could stimulate this program via the transcriptional coactivator PGC-1α and possibly via ERRγ/β.

an increase in slow oxidative fiber composition and vascularity in mice (14, 22, 29–31). Herein, we show that PPARβ/δ and ERRγ function to activate transcription of the *Myh7* and *Myh7b* genes, increasing the levels of miR-208b and miR-499 and, thereby, triggering a cascade of muscle slow-twitch contractile protein gene expression (19, 20). The related nuclear receptor PPARα suppresses the activating effects of PPARβ/δ/ERRγ on *Myh7/miR-208b* and *Myh7b/miR-499*.

Muscle endurance is determined by multiple factors, including capacity for mitochondrial fuel oxidation and ATP synthesis, fiber-type mix, and vascularity (1–3). The inducible transcriptional coactivator PGC-1α was shown previously to coordinately trigger these programs in muscle-specific transgenic mice (13). Thereafter, muscle transgenes for PPARβ/δ and ERRγ, known transcription factor targets of PGC-1, were shown to exhibit a trained muscle phenotype, including increased expression of well-established PPAR/ERR target genes involved in mitochondrial energy transduction and oxidative phosphorylation, together with an increased proportion of type I fibers (14, 16, 22, 29–31). We sought to delineate the regulatory circuitry linking the activation of energy metabolic genes with the fiber-type program by taking advantage of the markedly different muscle phenotypes of the MCK-PPARα and MCK-PPARβ/δ lines. Using a combination of gene expression and miRNA profiling, we found that ERRγ/ERRβ and miR-208b/miR-499 levels were increased in parallel with expression of type I fiber genes in the muscle of MCK-PPARβ/δ mice. In striking contrast, miR-208b/miR-499 levels were suppressed in MCK-PPARα muscle, together with a lack of induction of ERRγ and ERRβ and suppression of the type I program. These results were intriguing given the recent discovery that miR-208b and miR-499 are embedded in slow-twitch MHC genes and serve to activate slow-twitch fiber program by downregulating the expression of transcriptional repressors, including *Sox6* and *Purb*, which, in turn, suppress slow-twitch genes (19, 20, 32–36).

We found that ERRγ serves a critical role in this regulatory network by directly activating transcription of the *Myh7* (*miR-208b*) and *Myh7b* (*miR-499*) genes via highly conserved ERR-responsive elements. The expression of ERRγ and the related ERRβ (but not ERRα) is elevated in MCK-PPARβ/δ muscle through mechanisms that remain unknown. Interestingly, the results of our studies using myotubes in culture suggest that activation of the type I fiber program by PPARβ/δ occurs via a ligand-independent mechanism (data not shown). The mouse ERRγ has at least two different promoters. We have found that the activity of both promoters is increased in MCK-PPARβ/δ muscle, with the transcript driven by the downstream promoter exhibiting the greatest increase in MCK-PPARβ/δ muscle (data not shown). Using informatics search approaches, we have not been able to identify conserved PPAR binding motifs (37, 38) in potential regulatory regions in the DNA sequence spanning from approximately –100 kb upstream to approximately 50 kb downstream of the ERRγ downstream promoter transcription initiation site. Thus, we conclude that activation of ERRγ by PPARβ/δ likely occurs via an indirect mechanism. In addition, it is possible that PPARβ/δ and ERRγ interact at other levels, including, but not limited to, cooperating (directly or indirectly) to activate transcription of type I fiber genes. Our results also suggest that the ERRγ/β-driven muscle fiber-type program does not require the transcriptional coactivator PGC-1α, which has been shown to regulate fiber type, likely in response to endurance training (13, 39–43). However, it would seem likely that with certain physiological conditions, such as exercise, induction of PGC-1 could further enhance the mechanism described herein by coactivating PPARβ/δ. Taken together, our results suggest the existence of a regulatory network, as shown in Figure 8.

Muscle fiber-type proportion is determined by both fundamental developmental mechanisms and postnatal physiological stimuli, such as exercise training (1–3). The tissue-selective promoters used in the generation of gain-of-function (PPAR transgene) and loss-of-function (*Esrrg/Esrrb* gene knockout) mouse lines for this study are both active during prenatal development, suggesting that the mechanisms described may be capable of driving fundamental fiber-type determination. However, the results of our CLFS studies in cell culture indicate that this nuclear receptor/miRNA regulatory circuit is inducible. Interestingly, we found that ERRγ is required for the CLFS-triggered induction of this program. In addition, our survey of the human muscle samples also demonstrated that the ERRγ/miR-499 circuit was activated in the "active" group. Specifically, *ESRRG* and miR-499 levels were higher in muscle samples obtained from trained "active" individuals compared with those of sedentary individuals. We also found that the expression of *ESRRG* and miR-499 was strongly correlated with fiber-type proportion, expression of *MYH7* and *MYH7B* genes, and measures of enhanced exercise performance (including VO_{2max}). However, we did not see similar correlations with *PPARD* or *PPARA* expression in humans. This could relate to species differences. Alternatively, the programs directed by *PPARA* and *PPARD* in humans may not be manifest in the "active"-versus-sedentary group comparison, because this pathway is primarily involved in other genetic programs (e.g., fundamental developmental programs). Given that we did not conduct a longitudinal training study in humans or mice, our results do not allow us to determine whether this regulatory

pathway is involved in the response to endurance training or determination of fundamental fiber type during development. Obviously, these are not mutually exclusive roles, and future studies will be necessary to further delineate the function of this pathway in response to physiological inputs.

The upstream regulatory mechanisms that link inputs, such as developmental cues or exercise, to the network defined here are unknown. Evidence has emerged that exercise induces a switch in the relative abundance of transcriptional corepressor complexes, such as the nuclear receptor corepressor 1/histone deacetylase (NCoR1/HDAC) (44, 45) complex, and coactivator complexes containing inducible factors, such as PGC-1α (13, 39–43), at the regulatory regions of key genes that control muscle mitochondrial function and fiber type. Interestingly, NCoR1/HDAC– and PGC-1α–containing cofactor complexes are known to corepress or coactivate ERRs (44, 46, 47) and PPARs (44, 47, 48), respectively, thereby suggesting a mechanism whereby the pathways described here could be dynamically modulated. In addition, the transcriptional coregulator MED13 was recently shown to control metabolism downstream of miR-208a in heart, suggesting additional potential control mechanisms (49).

Surprisingly, in contrast to miR-499, miR-208b levels were not higher in the "active" muscle compared with those in control. The reason for this difference compared with the results in the mouse lines is not clear. This could reflect a species-specific posttranscriptional regulatory effect. Indeed, evidence is emerging that RNA processing, including but not limited to alternative splicing and RNA degradation, are highly active and regulated in muscle. It is tempting to speculate that such mechanisms are active in human muscle such that the miR-208b steady-state levels are not increased in humans.

In summary, we have identified a gene regulatory pathway, involving nuclear receptor and miRNA signaling, which is involved in the coordinate control of muscle energy metabolism and fiber type. Increased proportion of type I fibers and enhanced mitochondrial function are linked to improved glucose tolerance and insulin sensitivity (6–9). Conversely, obesity and chronic disease states, such as heart failure, result in detrained muscle, with reduced numbers of oxidative muscle fibers and diminished fuel-burning capacity. Therefore, the regulatory network described here shows promise as a candidate target for new therapeutic approaches aimed at coordinately increasing muscle type I fibers and energy metabolic capacity.

Methods

Animal studies. *Esrrg*- and *Esrrb*-floxed (ERRγ/ERRβ$^{L2/L2}$) mice were generated at the Mouse Clinical Institute in Strasbourg according to a strategy previously described (44) and back-crossed to the C57BL/6JBomTac background for 10 generations. To generate mice with skeletal muscle–specific deletions of the ERRγ/ERRβ alleles (herein referred to as ERRβ/γ dmKO mice), ERRγ/ERRβ$^{L2/L2}$ mice were crossed to human skeletal actin–Cre (HSA-Cre) mice. PPARα-null (*Ppara*$^{-/-}$) mice in the C57BL/6J background were purchased from The Jackson Laboratory (stock no. 008154). High-expressing (HE) MCK-PPAR mice have been previously described (16, 17). C3B6F1 MCK-miR-499 mice (19) were bred with MCK-PPARα mice to generate the MCK-PPARα/miR-499 double-transgenic mice. The MCK-PPARα mice are in a C57BL/6J pure strain and MCK-PPARβ/δ mice are in a hybrid B6/CBA background, with the following specific exceptions: hybrid MCK-PPAR mouse lines were used in Figure 3 (C3/B6) and Supplemental Table 1 (B6/CBA). NTG littermate controls were used in all cases. Of note, fiber-type analyses confirmed that the fiber-type switch phenotype was similar in pure B6 mice compared with that in the hybrid MCK-PPAR mice (data not shown).

Human studies. Details on subject characteristics and procedures have been described previously (27) and are provided in Supplemental Table 2. Briefly, mitochondrial capacity, as measured by ATP_{max}, was determined on a 3T GE Signa MNS magnet (GE) using a 4- or 6-cm ^{31}P-tuned surface coil positioned over the distal vastus lateralis. For maximum aerobic capacity (VO_{2max}), cardiorespiratory testing was conducted in the Exercise Testing Core, using a standardized graded exercise testing protocol on a stationary bicycle ergometer (Lode Excalibur). After an overnight fast and local anesthesia, skeletal muscle was collected from the vastus lateralis muscle, cleaned, and mounted for fiber typing as described previously (27) or flash frozen in liquid nitrogen for RNA isolation.

Exercise studies. Endurance exercise was determined as described previously (16) with the following exception. Fed mice were run for 10 minutes at 10 meters per minute followed by a constant speed of 20 meters per minute until exhaustion. For assessment of ERRβ/γ dmKO mouse running capacity, mice were run for 45 minutes at 15 meters per minute at 5% incline, followed by an increase of 2 meters per minute every 15 minutes until exhaustion (defined as remaining on the shock grid for more than 1 minute).

Histologic analyses. Muscle tissue was frozen in isopentane that had been cooled in liquid nitrogen. MHC ATPase and immunofluorescence stains were conducted as previously described (39, 50). MHC ATPase stains were performed at pH 4.31. Under these acidic conditions, MHC2 isoforms are inactivated while MHC1 is still functional, resulting in addition of black dye to MHC1-positive muscle fibers. For immunofluorescence stains, the fibers were quantified (MHC1, green; MHC2a, blue; MHC2x, black [unstained]; MHC2b, red) and expressed as relative numbers of the different fiber types.

TLDA array. Total RNA isolated from soleus muscles of 3-month-old MCK-PPARα (HE) or MCK-PPARβ/δ (HE) mice and NTG littermates using the RNAzol method (Tel-Test) was used for the gene expression array. TaqMan Rodent microRNA Arrays v2.0 (A and B) (Applied Biosystems) were performed by the Sanford-Burnham Medical Research Institute Analytical Genomics Core. For miRNA cDNA synthesis, 1 μg RNA was reverse transcribed using the miRNA Reverse Transcription Kit in combination with the stem-loop Megaplex Primer Pool (Applied Biosystems) in a total of 7.5 μl volume. Quantitative real-time PCR was performed using the Applied Biosystems 7900HT system and a TaqMan Universal PCR Master Mix, with 6 μl cDNA input per plate using the following conditions: 10 minutes at 94.5°C followed by 40 cycles of 97°C for 30 seconds and 59.7°C for 1 minute. Real-Time StatMiner Software from Integromics was used for the data analysis, and mouse snoRNA202 was used as endogenous control for data correction. Ct values greater than 30 in both NTG and MCK-PPAR mice were excluded. Fold change was calculated by the $2^{-\Delta\Delta Ct}$ method using averaged values from 3 trials. The relative miRNA level was normalized to NTG control. A moderated *t* test was performed to identify significance, as defined by the following criteria: *P* value less than 0.01 and fold change greater than 2 (either direction).

RNA analyses. Real-time quantitative RT-PCR was performed as described previously (16). Specific oligonucleotide primers for target gene sequences are listed in Supplemental Table 3. Arbitrary units of target mRNA were corrected to expression of *36b4* or *GAPDH*. The gene expression array and miRNA array data have been deposited in NCBI's Gene Expression Omnibus (GEO) and are accessible through GEO accession numbers GSE5777, GSE29055, and GSE36498 (miRNA array).

TaqMan miRNA. Total RNA was isolated from mouse muscle or primary myotubes using the RNAzol method (Tel-Test) for miRNA assay. Total RNA from human muscle biopsy specimens was extracted using the RNeasy Mini Kit and the miRNeasy Mini Kit (Qiagen). TaqMan methods were used to assess miRNA expression. Briefly, 10 ng RNA (for skeletal

muscle) or 50 ng RNA (for primary myotubes) was reverse transcribed to cDNA with the TaqMan MicroRNA Reverse Transcription Kit and the TaqMan MicroRNA Assays specific for each miRNA (Assay ID: hsa-miR-208b, 2290; mmu-miR-499, 1352; has-miR-499, 1045) or for the internal controls (Assay ID: snoRNA202, 1232; RNU48, 1006) (Applied Biosystems). Thermal cycling was performed on an Applied Biosystems 7900HT system. The relative miRNA level was corrected to snoRNA202 or RNU48.

Antibodies and immunoblotting studies. Antibodies directed against MHC1 (BA-D5), MHC2b (BF-F3), and MHC2a (SC-71) were purchased from the Developmental Studies Hybridoma Bank; anti-ERRγ antibody was provided by Ronald Evans (Salk Institute for Biological Studies, San Diego, California, USA); anti-GAPDH antibody was purchased from Abcam; antibody directed against S6 ribosomal protein (S6RP) was purchased from Cell Signaling Technology. Western immunoblotting studies were performed as previously described (16).

Cell culture. Primary muscle cells were isolated from skeletal muscles as previously described (16). C2C12 cells were cultured at 37°C and 5% CO_2 in Dulbecco's modified Eagle's medium supplemented with 10% fetal calf serum. For differentiation, cells were washed with PBS and refed with 2% horse serum/DMEM differentiation medium and refed daily. Primary myoblasts were infected with an adenovirus overexpressing GFP, PPARβ/δ, PPARα, ERRγ, GFP shRNA, or PPARβ/δ shRNA as previously described (16, 51). Twelve hours after infection, cells were induced to differentiation for 3 days.

Electric pulse stimulation. CLFS was applied to primary mouse myotubes with a S88X stimulator (Grass Technologies). This instrument provides a positive phase followed by a negative phase of identical duration and voltage. During the 1-s trains, a 200-ms pulse stimulus with 2.5 V and a frequency of 2 Hz was applied. The contractions of the myotubes were verified by examination under microscope. Primary myotubes were stimulated for 4 hour per day for 4 days.

Manipulation of miR-208b and miR-499 in primary skeletal myotubes. For inhibition of miR-208b and/or miR-499, validated miRCURY LNA microRNA Power Inhibitors (has-miR-499-5p: ACATCACTGCAAGTCTT; has-miR-208b: ACAAACCTTTTGTTCGTCTT; and a negative control A: GTGTAACACGTCTATACGCCCA) were purchased from Exiqon and transfected into primary myoblasts at a final concentration of 20 to 50 nM using HiPerFect Transfection Reagent (Qiagen) according to the manufacturer's instructions. Twelve hours after transfection, cells were induced to differentiation for 3 days.

RNAi experiments. siRNAs (ON-TARGET plus SMARTpool, Dharmacon) targeting mouse *Esrrg* were transfected into primary myoblasts at a final concentration of 20 nM using HiPerFect Transfection Reagent (Qiagen) according to the manufacturer's instructions. Cells were then differentiated for 3 days prior to harvest.

Cell transfection and luciferase reporter assays. pSG5, pSG5-ERRβ, pSG5-ERRγ, pBOS, pBOS-PPARα, pcDNA3.1, and pcDNA3.1-PGC-1α vectors have been described previously (16, 52). The 1.0-kb mouse *Myh7b* promoter-reporter (32) vector was provided by Leslie Leinwand (University of Colorado, Boulder, Colorado, USA). The rat *Myh7* promoter constructs (53) were provided by Kenneth Baldwin (University of California, Irvine, California, USA). Site-directed mutagenesis was performed using the QuikChange Kit (Stratagene) according to the manufacturer's protocol, using complementary oligonucleotides as follows (with mutated nucleotides shown in bold and with lowercase letters): 5′-GCTGTTGTCA**gatct**AGCAAAGGAG (*Myh7b* ERRmut). Transient transfections in primary myoblasts or C2C12 cells were performed using Attractene Transfection Reagent (Qiagen) as per the manufacturer's protocol. Luciferase assay was performed using Dual-Glo (Promega) according to the manufacturer's recommendations. All transfection data are presented as the mean ± SEM for at least 3 separate transfection experiments performed in triplicate.

ChIP assays. ChIP assays were performed as previously described (16). Briefly, primary myotubes were cross-linked with 1% formaldehyde (10 minutes), and cells were collected and lysed. Chromatin fragmentation was performed by sonication using a Bioruptor (Diagenode). Proteins were immunoprecipitated by using anti-ERRγ or IgG control (Sigma-Aldrich). Following reversal of crosslinking, DNA was isolated (QIAquick PCR Purification Kit, Qiagen). QPCR products were assessed and measured using the Stratagene MX3005P detection system. Quantitative analysis was performed by the standard curve method. Specific oligonucleotide primers for target regions are listed in Supplemental Table 4.

Statistics. All mouse and cell studies were analyzed by 2-tailed Student's *t* test or 1-way ANOVA coupled to a Fisher's least significant difference post-hoc test when more than 2 groups were compared. Data represent the mean ± SEM, with a statistically significant difference defined as $P < 0.05$. Statistical analyses in human studies were performed using JMP 9.0.0 (SAS Institute Inc.), and values are presented as mean ± SEM. Gene expression levels in human studies were analyzed using the Spearman correlation or Pearson correlation test. Significant differences were defined as $P < 0.05$.

Study approval. After signing the informed written consent approved by the Pennington Biomedical Research Center (PBRC) ethical review board, patients were enrolled the in clinical trial performed in Baton Rouge, Louisiana, USA, at the PBRC. Volunteers qualified for the study (ACTIV; Clinicaltrials.gov ID NCT00401791) if they ranged in age from 20 to 40 years, had a BMI of 20 to 30 kg/m^2, were nondiabetic, took no medications, and were otherwise healthy. Animal studies were conducted in strict accordance with the NIH guidelines for humane treatment of animals and approved by the IACUC committees at Sanford-Burnham Medical Research Institute at Lake Nona and The Scripps Research Institute at La Jolla.

Acknowledgments

This work was supported by NIH grants RO1DK045416 (to D.P. Kelly), R01AR41928 (to K.E. Conley), R01AG030226 (to S.R. Smith), and R01DK095686 (to A. Kralli) and a postdoctoral fellowship (11POST7420013) from the American Heart Association (to Z. Gan). E.N. Olson was supported by grants from the Robert A. Welch Foundation, the American Heart Association, Jon Holden DeHaan Foundation, and the Fondation Leducq TransAtlantic Network of Excellence in Cardiovascular Research Program. J. Auwerx was supported by grants from the ERC, the Ecole Polytechnique Fédérale de Lausanne, and the Swiss National Science Foundation. S.R. Smith was supported by Novartis Clinical Innovation Fund. Special thanks to Leslie Leinwand (University of Colorado) for providing the 1.0-kb mouse *Myh7b* promoter-reporter vector, Ronald Evans (Salk Institute for Biological Studies) for the anti-ERRγ antibody, Sudip Bajpeyi (PBRC) for the initial characterization of the human muscle samples, and the Analytical Genomics Core and the Histology Core at Sanford-Burnham Medical Research Institute at Lake Nona. We are grateful for Lorenzo Thomas for assistance with manuscript preparation, Xiaoman Li (University of Central Florida) for help with bioinformatics analyses, and Lauren Ashley Gabriel for assistance with animal studies.

Received for publication November 2, 2012, and accepted in revised form March 8, 2013.

Address correspondence to: Daniel P. Kelly, Sanford-Burnham Medical Research Institute at Lake Nona, 6400 Sanger Road, Orlando, Florida 32827, USA. Phone: 407.745.2136; Fax: 407.745.2034; E-mail: dkelly@sanfordburnham.org.

1. Booth FW, Thomason DB. Molecular and cellular adaptation of muscle in response to exercise: perspectives of various models. *Physiol Rev*. 1991; 71(2):541–585.
2. Hawley JA, Holloszy JO. Exercise: it's the real thing! *Nutr Rev*. 2009;67(3):172–178.
3. Yan Z, Okutsu M, Akhtar YN, Lira VA. Regulation of exercise-induced fiber type transformation, mitochondrial biogenesis, and angiogenesis in skeletal muscle. *J Appl Physiol*. 2011;110(1):264–274.
4. Schiaffino S, Reggiani C. Fiber types in mammalian skeletal muscles. *Physiol Rev*. 2011;91(4):1447–1531.
5. Pette D, Staron RS. Myosin isoforms, muscle fiber types, and transitions. *Microsc Res Tech*. 2000; 50(6):500–509.
6. Lillioja S, et al. Skeletal muscle capillary density and fiber type are possible determinants of in vivo insulin resistance in man. *J Clin Invest*. 1987; 80(2):415–424.
7. Henriksen EJ, et al. Glucose transporter protein content and glucose transport capacity in rat skeletal muscles. *Am J Physiol Endocrinol Metab*. 1990; 259(4 pt 1):E593–E598.
8. Song XM, et al. Muscle fiber type specificity in insulin signal transduction. *Am J Physiol*. 1999; 277(6 pt 2):R1690–R1696.
9. Daugaard JR, et al. Fiber type-specific expression of GLUT4 in human skeletal muscle: influence of exercise training. *Diabetes*. 2000;49(7):1092–1095.
10. Holloszy JO. Regulation by exercise of skeletal muscle content of mitochondria and GLUT4. *J Physiol Pharmacol*. 2008;59(suppl 7):5–18.
11. Saltin B, Henriksson J, Nygaard E, Andersen P, Jansson E. Fiber types and metabolic potentials of skeletal muscles in sedentary man and endurance runners. *Ann N Y Acad Sci*. 1977;301:3–29.
12. Zierath JR, Hawley JA. Skeletal muscle fiber type: influence on contractile and metabolic properties. *PLoS Biol*. 2004;2(10):e348.
13. Lin J, et al. Transcriptional co-activator PGC-1 alpha drives the formation of slow-twitch muscle fibres. *Nature*. 2002;418(6899):797–801.
14. Wang YX, et al. Regulation of muscle fiber type and running endurance by PPARδ. *PLoS Biol*. 2004; 2(10):e294.
15. Narkar VA, et al. AMPK and PPARδ agonists are exercise mimetics. *Cell*. 2008;134(3):405–415.
16. Gan Z, et al. The nuclear receptor PPARbeta/delta programs muscle glucose metabolism in cooperation with AMPK and MEF2. *Genes Dev*. 2011; 25(24):2619–2630.
17. Finck BN, et al. A potential link between muscle peroxisome proliferator- activated receptor-alpha signaling and obesity-related diabetes. *Cell Metab*. 2005;1(2):133–144.
18. Small EM, Olson EN. Pervasive roles of microRNAs in cardiovascular biology. *Nature*. 2011; 469(7330):336–342.
19. van Rooij E, et al. A family of microRNAs encoded by myosin genes governs myosin expression and muscle performance. *Dev Cell*. 2009;17(5):662–673.
20. Quiat D, et al. Concerted regulation of myofiber-specific gene expression and muscle performance by the transcriptional repressor Sox6. *Proc Natl Acad Sci U S A*. 2011;108(25):10196–10201.
21. Baldwin KM, Haddad F. Effects of different activity and inactivity paradigms on myosin heavy chain gene expression in striated muscle. *J Appl Physiol*. 2001;90(1):345–357.
22. Narkar VA, et al. Exercise and PGC-1alpha-independent synchronization of type I muscle metabolism and vasculature by ERRγ. *Cell Metab*. 2011; 13(3):283–293.
23. Dufour CR, et al. Genome-wide orchestration of cardiac functions by the orphan nuclear receptors ERRα and γ. *Cell Metab*. 2007;5(5):345–356.
24. Wehrle U, Dusterhoft S, Pette D. Effects of chronic electrical stimulation on myosin heavy chain expression in satellite cell cultures derived from rat muscles of different fiber-type composition. *Differentiation*. 1994;58(1):37–46.
25. Donoghue P, Doran P, Dowling P, Ohlendieck K. Differential expression of the fast skeletal muscle proteome following chronic low-frequency stimulation. *Biochim Biophys Acta*. 2005;1752(2):166–176.
26. Burch N, et al. Electric pulse stimulation of cultured murine muscle cells reproduces gene expression changes of trained mouse muscle. *PLoS One*. 2010; 5(6):e10970.
27. Bajpeyi S, et al. Skeletal muscle mitochondrial capacity and insulin resistance in type 2 diabetes. *J Clin Endocrinol Metab*. 2011;96(4):1160–1168.
28. Desvergne B, Wahli W. Peroxisome proliferator-activated receptors: nuclear control of metabolism. *Endocr Rev*. 1999;20(5):649–688.
29. Luquet S, et al. Peroxisome proliferator-activated receptor delta controls muscle development and oxidative capability. *FASEB J*. 2003;17(15):2299–2301.
30. Schuler M, et al. PGC1alpha expression is controlled in skeletal muscles by PPARβ, whose ablation results in fiber-type switching, obesity, and type 2 diabetes. *Cell Metab*. 2006;4(5):407–414.
31. Rangwala SM, et al. Estrogen-related receptor gamma is a key regulator of muscle mitochondrial activity and oxidative capacity. *J Biol Chem*. 2010; 285(29):22619–22629.
32. Bell ML, Buvoli M, Leinwand LA. Uncoupling of expression of an intronic microRNA and its myosin host gene by exon skipping. *Mol Cell Biol*. 2010; 30(8):1937–1945.
33. Hagiwara N, Ma B, Ly A. Slow and fast fiber isoform gene expression is systematically altered in skeletal muscle of the Sox6 mutant, p100H. *Dev Dyn*. 2005;234(2):301–311.
34. Hagiwara N, Yeh M, Liu A. Sox6 is required for normal fiber type differentiation of fetal skeletal muscle in mice. *Dev Dyn*. 2007;236(8):2062–2076.
35. Ji J, et al. Puralpha and Purbeta collaborate with Sp3 to negatively regulate beta-myosin heavy chain gene expression during skeletal muscle inactivity. *Mol Cell Biol*. 2007;27(4):1531–1543.
36. von Hofsten J, et al. Prdm1- and Sox6-mediated transcriptional repression specifies muscle fibre type in the zebrafish embryo. *EMBO J*. 2008;9(7):683–689.
37. Nielsen R, et al. Genome-wide profiling of PPARgamma: RXR and RNA polymerase II occupancy reveals temporal activation of distinct metabolic pathways and changes in RXR dimer composition during adipogenesis. *Genes Dev*. 2008;22(21):2953–2967.
38. Adhikary T, et al. Genomewide analyses define different modes of transcriptional regulation by peroxisome proliferator-activated receptor-β/δ (PPARβ/δ). *PLoS One*. 2011;6(1):e16344.
39. Zechner C, et al. Total skeletal muscle PGC-1 deficiency uncouples mitochondrial derangements from fiber type determination and insulin sensitivity. *Cell Metab*. 2010;12(6):633–642.
40. Baar K, et al. Adaptations of skeletal muscle to exercise: rapid increase in the transcriptional coactivator PGC-1. *FASEB J*. 2002;16(14):1879–1886.
41. Finck BN, Kelly DP. PGC-1 coactivators: inducible regulators of energy metabolism in health and disease. *J Clin Invest*. 2006;116(3):615–622.
42. Goto M, et al. cDNA Cloning and mRNA analysis of PGC-1 in epitrochlearis muscle in swimming-exercised rats. *Biochem Biophys Res Commun*. 2000; 274(2):350–354.
43. Pilegaard H, Saltin B, Neufer PD. Exercise induces transient transcriptional activation of the PGC-1α gene in human skeletal muscle. *J Physiol*. 2003; 546(pt 3):851–858.
44. Yamamoto H, et al. NCoR1 is a conserved physiological modulator of muscle mass and oxidative function. *Cell*. 2011;147(4):827–839.
45. Potthoff MJ, et al. Histone deacetylase degradation and MEF2 activation promote the formation of slow-twitch myofibers. *J Clin Invest*. 2007; 117(9):2459–2467.
46. Huss JM, Kopp RP, Kelly DP. Peroxisome proliferator-activated receptor coactivator-1alpha (PGC-1α) coactivates the cardiac-enriched nuclear receptors estrogen-related receptor-α and -γ. Identification of novel leucine-rich interaction motif within PGC-1α. *J Biol Chem*. 2002;277(43):40265–40274.
47. Huss JM, Kelly DP. Nuclear receptor signaling and cardiac energetics. *Circ Res*. 2004;95(6):568–578.
48. Vega RB, Huss JM, Kelly DP. The coactivator PGC-1 cooperates with peroxisome proliferator-activated receptor alpha in transcriptional control of nuclear genes encoding mitochondrial fatty acid oxidation enzymes. *Mol Cell Biol*. 2000;20(5):1868–1876.
49. Grueter CE, et al. A cardiac microRNA governs systemic energy homeostasis by regulation of MED13. *Cell*. 2012;149(3):671–683.
50. Waters RE, Rotevatn S, Li P, Annex BH, Yan Z. Voluntary running induces fiber type-specific angiogenesis in mouse skeletal muscle. *Am J Physiol Cell Physiol*. 2004;287(5):C1342–C1348.
51. Kleiner S, et al. PPAR{delta} agonism activates fatty acid oxidation via PGC-1{alpha} but does not increase mitochondrial gene expression and function. *J Biol Chem*. 2009;284(28):18624–18633.
52. Huss JM, Torra IP, Staels B, Giguere V, Kelly DP. Estrogen-related receptor alpha directs peroxisome proliferator-activated receptor alpha signaling in the transcriptional control of energy metabolism in cardiac and skeletal muscle. *Mol Cell Biol*. 2004; 24(20):9079–9091.
53. Wright CE, Haddad F, Qin AX, Bodell PW, Baldwin KM. In vivo regulation of beta-MHC gene in rodent heart: role of T3 and evidence for an upstream enhancer. *Am J Physiol*. 1999;276(4 pt 1):C883–C891.